

1 Criticality in the planform behavior of the Ganges River  
2 meanders

3 **P.A. Carling<sup>1</sup>, N. Gupta<sup>2</sup>, P.M. Atkinson<sup>1,3</sup>, and Huang Qing He<sup>4</sup>**

4 <sup>1</sup>*Geography and Environment Department, University of Southampton, Southampton*  
5 *SO17 1BJ, UK*

6 <sup>2</sup>*Tea Research Association, Jorhat 785008, India*

7 <sup>3</sup>*Faculty of Science and Technology, Lancaster University, Lancaster LA1 4YW, UK*

8 <sup>4</sup>*Chinese Academy of Sciences, 100864 Beijing, China*


9 **ABSTRACT**

10 The critical point of planform transition from straight to meandering in the  
11 wandering Ganges River is identifiable. Recent remote-sensing data indicate that four  
12 similar meanders cut off, or attempted to cut off, after ~31–35 yr, primarily due to  
13 channel aggradation. As main channels aggrade, sinuosity is maximized for broad  
14 channel widths and small radii of curvature and relaxes for bends of greater radii.  
15 Maximized form resistance occurs close to self-organized criticality and promotes  
16 cutoffs. Avulsions lead to main channel narrowing and prevent further bend  
17 tightening, relaxing the system by reducing sinuosity. Thus, the wandering river  
18 oscillates in space and time across the transition from a more ordered to a more  
19 chaotic state. Planform behavior is described by the Jerolmack-Mohrig mobility  
20 number and the Parker stability criterion, which well define meander behavior as they  
21 approach criticality and then relax via partial or completed avulsions. The results have  
22 significance for river engineering and river network and stratigraphic modeling. Such  
23 an approach could be of practical value when predicting the behaviors of other major  
24 wandering rivers.



25 **INTRODUCTION**

26 Stølum (1996) showed that channel sinuosity oscillates across a predictable  
27 critical state mediated by local cutoff (avulsion) processes. Such an adjustment is a  
28 form of self-organized criticality (SOC; Bak, 1996); when the critical state is reached,  
29 meanders adjust to regain order before evolving further. Using the criticality concept,  
30 we show that the course of the wandering Ganges River, India (study area:  
31 24.459317°N, 88.103924°E; Fig. 1), oscillates in space and time from a more ordered  
32 to a more chaotic state (Stølum, 1996), without change in the magnitude and  
33 frequency of external forcing. However, the SOC environment and time scale can be  
34 subject to local fixed controls (here bedrock pinch points) that condition SOC  
35 behavior (Camazine et al., 2001). The low-sinuosity river (ordered state) increases its  
36 sinuosity (chaotic state) until local bank instabilities, manifest as avulsions, lead to  
37 channel shortening to reach a low sinuosity value again. Meander regrowth follows.  
38 Thus, the critical state is defined as the planform pattern transition point.

39 Between Farakka Barrage (West Bengal, India) and Hardinge Bridge (Sara,  
40 Bangladesh), three meanders occur, with a further meander immediately upstream of  
41 the barrage (Fig. 1 **[[The figure does not identify the barrage or bridge – label  
42 these in the figure? 

Page 2 of 15**


50 decadal time scales that lead to periodic reduction in main channel length and  
51 sinuosity. In addition, 38 yr of remote sensing data (Landsat Multispectral Scanner,  
52 Thematic Mapper, Indian Remote Sensing Satellites Linear Imaging Self-Scanning  
53 [LISS] I and LISS III) (from 1972) were used to explore channel planform changes by  
54 identifying completed avulsions or partial avulsions (Fig. 1). Main channel widths and  
55 radii of curvature at meander apices were quantified for each of the four meanders  
56 through time.

## 57 **SETTING**

58       The annual peak flow on the Ganges River usually occurs within a 1.5 m stage  
59 range. Bankfull discharge is exceeded yearly, then the low natural levees are  
60 overtopped by shallow floodplain flow or are breached by small cutoffs that transect  
61 the major meander loops. These cutoffs scour the floodplains (Coleman, 1969), but  
62 the main channel does not realign. Rather, it takes several years for the main flow to  
63 adopt any enlarging cutoff channel (Fig. 1). Upstream of the Farakka Barrage the  
64 sediment load is  $729 \times 10^6 \text{ t yr}^{-1}$  (Wasson, 2003) which, due to the barrage, reduces  
65 downstream to  $300\text{--}500 \times 10^6 \text{ t yr}^{-1}$  at Hardinge Bridge (Hossain et al., 2013). The  
66 barrage (constructed in 1975) was fully aggraded by 1995 (Fig. 2), and much  
67 sediment now passes by canal to the Bhagirathi-Hooghly River. Thus, the sediment  
68 load downstream of the barrage reduces by  $\sim 41\text{--}68\%$ .

69       Four similar meander bends were studied (Fig. 1): one upstream (R1) and  
70 three downstream (R2–R4) of the barrage. All bends developed simultaneously and  
71 cut off, or attempted to cut off, by chute development over similar time scales (31–35  
72 yr). Thus, although the remote sensing time series is too short to develop a statistical  
73 assessment of cutoff frequency, there are four replicates of the cutoff phenomenon.

## 74 **CONDITIONS FOR AVULSION**

75 The avulsion condition largely is due to channel aggradation (Jerolmack and  
76 Mohrig, 2007) that forces overbank flows to occur more frequently. However,  
77 tightening bends deepen on their outer banks (Seminara, 2006), and increasing bend  
78 flow resistance causes both elevation in the outer bank flow level and increased bank  
79 erosion, which increases [[Corre ]] channel width (Germanoski and Schumm,  
80 1993). These conditions jointly are conducive to avulsion. Thus, the critical cutoff  
81 condition can be determined for each bend and depends on (1) channel geometry, (2)  
82 discharge, and (3) aggradation rate.

### 83 **Channel Geometry**

84 The radius of curvature ( $r$ ) was determined for each of the main channel  
85 bends. The radii of curvature decreased through time, whereas the channel widths ( $B$ )  
86 often increased (Hossain et al., 2013). The inability of point bar progradation to match  
87 the rate of bend apex recession, such that  $B$  increases as bends tighten, has been noted  
88 elsewhere (Kasvi et al., 2015). The condition preceding a completed (or attempted)  
89 cutoff and a sudden decrease in sinuosity ( $S$ ) occurred when the bend radius fell to  
90 between 5000 m and 2000 m. Thus, cutoff likelihood, in part, can be defined by the  
91 ratio  $r/B$  (Howard and Knutson, 1984). To cut off, the river must flow overbank and  
92 avulse by rapid erosion of the levee and floodplain surface. The minimum condition  
93 for overbank flow is bankfull discharge (van Dijk et al., 2014) plus super-elevated  
94 outer bank flow. For bankfull flow ( $Q_b \sim 56,633 \text{ m}^3 \text{ s}^{-1}$ ; Coleman, 1969), for the  
95 channel width ( $\sim 4000 \text{ m}$ ) immediately before cutoff occurs, and for the minimum  
96 radius of curvature (2000 m), the water surface super-elevation ( $\Delta y$ ) is:

$$97 \quad \Delta y = \frac{c\bar{U}^2\bar{B}}{rg}, \quad (1)$$

98 where  $c$  is a coefficient (0.5) for subcritical flows, the bankfull bulk-flow velocity  
99  $\bar{U} = Q_b/\bar{h}\bar{B}$ , where  $\bar{B}$  and  $\bar{h}$  are average values of the channel width and depth ( $h$ )

100 at bankfull, and  $g$  is **acceleration due to** gravity. Bankfull velocity is low (on the order  
101 of  $1 \text{ m s}^{-1}$ ) such that inertia is small. Thus, super-elevation at the bankline is no more  
102 than  $\sim 50$  mm above the channel center water surface. So, for these shallow overbank  
103 conditions, near-bankfull flows alone are not likely to induce cutoff (Howard, 2009).  
104 Rather, sustained outer-bank erosion, causing  $r/B$  to continue to decrease and further  
105 channel aggradation, is required to elevate water levels additionally. Alternatively,  
106 discharges much above bankfull are required.

### 107 **Discharge**

108 Rapid erosion of the outside bend will occur if discharge is adequate to entrain  
109 bank material for a sufficient time (Edmonds et al., 2009). Bendway flow resistance  
110 will reach a maximum as the radius of curvature reaches a minimum value. The  
111 straight channel shear stress ( $\tau_T$ ) due to skin friction ( $f$ ) is:

$$112 \quad \tau_T = \rho g R S_e = \rho f \bar{U}^2, \quad (2)$$

113 where  $\rho$  is the density of water,  $R$  is the hydraulic radius, and  $S_e$  is the energy slope.

114 The hydraulic radius is  $\sim 16$  m with a regional bankfull  $S_e$  of  $5\text{--}6 \times 10^{-5}$  (Coleman,  
115 1969). These data provide an estimate of unit shear stress on the order of  $10 \text{ N m}^{-2}$ .

116 Determining additional form resistance induced by bends is complex (e.g., Chang,  
117 1983). However, for illustrative purposes, we utilize the method of Leopold et al.

118 (1960) to estimate bend form shear stress ( $\tau_B = \rho g \bar{h} S_\zeta$ ) using an energy dissipation  
119 term ( $\bar{h} S_\zeta$ ):

$$120 \quad \bar{h} S_\zeta = \frac{\bar{U}^2}{g} \left( \frac{B}{r} - 0.5 \right) - h(1 + 1.5F^{0.66}), \quad (3)$$

121 where  $F$  is the near-bank Froude number for given local depth  $h$ . For the minimum  
122 values of  $r/B$ , the form-induced shear stress can be up to an order of magnitude larger  
123 than the skin shear stress. For greater  $r/B$  values, the form resistance declines. When

124 avulsions were imminent, values of  $r/B$  are consistent for all four reaches ( $\overline{1.29}$ ,  
125 standard deviation 0.72;  $n = 27$ ) but smaller than those values ( $\sim 3$ ) reported by Begin  
126 (1986) and Howard and Knutson (1984) for the condition when bank retreat through  
127 erosion is maximized. Thus, the ability of the channel to develop significant form  
128 resistance and adjust through increasing sinuosity is maximized for small radii of  
129 curvature and decreases for bends of greater amplitude. However, increasing form  
130 resistance as bends tighten induces a backwater effect and super-elevation that is  
131 conducive to cutoff before  $r/B$  is maximized, preventing further bend tightening and  
132 relaxing the system by reducing sinuosity.

### 133 **Aggradation**

134 The aggradation rates for meander bends R2–R4 are unknown, but for R1,  
135 channel aggradation and subsequent attempted avulsion were induced by backwater  
136 sedimentation above the barrage. A linear and then asymptotic approach to constant  
137 zero aggradation is typical of impoundments (Wu et al., 2012) and provides a  
138 maximum aggradation rate,  $\sim 0.18 \text{ m yr}^{-1}$ , to use as a scalar in R1 (Fig. 2A). Bend  
139 extension increases rapidly once one-third of the impoundment depth is filled (Fig.  
140 2B). For R2–R4, the aggradation rate ( $V_a$ ) is assumed to be proportional to the  
141 reduction in the sediment load ( $V_a = 300/729 \times 0.18 \text{ m yr}^{-1}$ ) below the Farakka  
142 Barrage. As the system aggraded, channel sinuosity increased, and attempted  
143 avulsions and cutoffs developed (Figs. 2 and 3). As ~~channel aggradation rate,~~  
144  $T_A$  **[[Clarify how this differs from  $V_a$ ]]**, mediates the ~~rate of lateral erosion,~~  $T_C$ , the  
145 latter a key variable to define critical state (Stølum, 1998), consideration of  $T_A:T_C$  can  
146 define the critical state of the planform pattern transition if other factors are  
147 significantly subordinate.


### 148 **PLANFORM SCALING MODEL**

149 The model used to show the meander behavior is the Jerolmack and Mohrig  
150 (2007) approach to calculate the avulsion frequency ( $f_A$ ) of a river. The avulsion  
151 frequency,

$$152 \quad f_A = \frac{V_a N}{\bar{h}}, \quad (4)$$

153 is known approximately. Each reach avulsed, or tried to avulse, at a time scale of  
154 ~31–35 yr, so  $f_A$  can be set to 0.03 for active channels  $N = 1-4$ , with an average  
155 channel depth of  $\bar{h} = 22$  m. Jerolmack and Mohrig (2007) developed a channel  
156 mobility number ( $M$ ) to discriminate single-channel versus multichannel form:

$$157 \quad M = \frac{T_A}{T_C} = \frac{\bar{h}}{B} \frac{V_c}{V_a}, \quad (5)$$

158 ~~where  $T_C$  is the time to migrate one channel~~  ~~th and  $V_c$  is the bank erosion rate.  $M =$~~   
159  $T_A/T_C = 1$  defines the critical planform pattern transition (Jerolmack and Mohrig,  
160 2007). The general trend of  $M$  in Figure 3 shows the temporal trajectories of reach  
161 behavior. For  $M \gg 1$ , a single, laterally mobile sinuous channel is expected. For  $M \approx$   
162 1, then transition is expected between a single channel and multiple channels. For  $M$   
163  $\ll 1$ , a multichannel avulsive system is expected. In accord with SOC, few, small  
164 avulsions release energy which suppresses the likelihood of large avulsions, whereas  
165 large avulsions increase the energy capacity of the network, which is a destabilization  
166 (Stølum, 1998). Accordingly, the network is attracted to  $M \approx 1$ . Such a simple model  
167 uses few parameters to elucidate emergent behavior without appeal to detailed  
168 process.

169  $M$  is used here with the Parker (1976) channel stability criterion ( $\varepsilon$ ),

$$170 \quad \varepsilon = S_e \sqrt{g \bar{h} B^4} / Q, \quad (6)$$

171 to define system trend through channel pattern phase space (Fig. 4), where  $Q$  is a  
172 formative discharge (bankfull value). A single-thread channel should dominate when

173  $\varepsilon \ll 1$ , while a braided form should be common for  $\varepsilon \geq 1$ . Jerolmack and Mohrig  
174 (2007) argued that a plot of  $M$  versus  $\varepsilon$  discriminated between planforms representing  
175 rivers *at a single point in time* across spatial scales. In contrast, we use the  $M$ - $\varepsilon$  phase  
176 space to explore meander bend evolutions *through time* as the channel morphology  
177 varies across the point of criticality due to hydraulic and morphological forcing. It is  
178 evident that meander R1 differs in its behavior in contrast to R2–R4, in that the Parker  
179 criterion for R1 lies between values of 0.6 and 1.5 while the other meanders exhibit  
180 values typically  $< 0.4$ . The values of  $M = 1$  and  $\varepsilon < 0.4$  define four quadrant phase  
181 spaces for channel planform discrimination (Fig. 4).

## 182 **DISCUSSION**

183 A power-law avulsion distribution may characterize SOC behavior but, as  
184 with many studies (Hooke, 2007), our reach length is inadequate for this test. In  
185 addition, a time constant is imposed on the Ganges' SOC cutoff behavior by spatial  
186 pinch points, such that cycling occurs, similar to other guided SOC phenomena  
187 (Prokopenko et al., 2014).

188 So, we focused on the critical state: defining avulsion as an autogenic response  
189 of a channel when it cannot adjust further through gradual variation of sinuosity  
190 (Stølum, 1996). As  $M$  approaches 1, there is an increased propensity for channel  
191 alignment to reset by cutoff to regain low sinuosity.

192 In a flume, lacking bank-stabilizing vegetation, cutoffs occurred at a small  
193 value of  $S \approx 1.2$ , preventing the development of more sinuous channels (Braudrick et  
194 al., 2009). The Ganges River also is vegetation free and tends to avulse when  $S$  is  $\sim 1.3$   
195 (Fig. 3). However, the situation is not simple, as a new avulsion relaxes the system  
196 such that both cutoff and main channel can be simultaneously active. There is not  
197 usually a simple abandonment of the main channel in favor of the new channel (Fig.



198 1). These “soft avulsions” (Edmonds et al., 2011) divert some discharge and sediment  
199 from the main channel (Coleman, 1969), but much load continues down the main  
200 channel. The effects of cutoffs on main channel response are poorly known  
201 (Seminara, 2006). However, as main channel discharge declines, deposition **occurs** in  
202 the main channel below the avulsion point, reducing channel width (Sorrells and  
203 Royall, 2014); the main thalweg depth is less affected as long as the main channel  
204 discharge remains greater than the cutoff discharge. The relaxation in the system, due  
205 to the soft avulsion, results in the main meander  $r/B$  increasing as  $B$  adjusts more  
206 readily than  $r$ , which sustains potential for bank erosion downstream of the avulsion  
207 as flow is increasingly confined by channel narrowing through time (Coleman, 1969).  
208 Thus, soft avulsion may assist a channel **in maintaining** its meandering habit and so  
209 delay a catastrophic reduction in sinuosity. Notwithstanding the relaxation due to  $B$ ,  $r$   
210 also increased in three of the meanders, preventing or delaying avulsion (Fig. 3).

211 Meander R1, influenced by **Farakka** Barrage backwater, cycles from  
212 anastomosed-braided to a single-channel braided pattern (Fig. 4). This pattern differs  
213 from **those of** R2–R4, which cycle from avulsive-anastomosed to a sinuous single-  
214 channel pattern, as is typical of wandering rivers. Thus, the imposition of the barrage,  
215 with consequent accelerated upstream aggradation **and** reductions in slope and  
216 channel depth, but broadening of the channel, caused a shift from a wandering to a  
217 braided pattern, as indexed by the values of  $\varepsilon$ . Thus, our analysis indicates that rapid  
218 aggradation in a wandering river (R1) leads to braiding (*viz.* Carson, 1984, his  
219 wandering type II). Moreover, the wandering planform is sustainable through time,  
220 with three meanders (R2–R4) adjusting similarly through time from meandering to a  
221 straighter main channel planform by the development of bend cutoffs. So, the  
222 wandering habit is not necessarily indicative of a channel in short-term transition

223 between single-channel meandering and braiding (Carson, 1984). To date, the  
224 reduction in sediment load downstream of the barrage has not changed the channel  
225 pattern, but a more stable meandering habit is predicted by Equation 5 (*viz.* Carson,  
226 1984, his wandering type I) and **has been** observed recently (Hossain et al., 2013).  
227 Consequently, a considerable time lag can be associated with any transition. The  
228 similar trend in behavior **among** all four meanders through similar time scales is  
229 highly significant in that criticality develops naturally in the meandering system.

230       Clearly, the meanders are affected by the barrage. Nevertheless, the boundary  
231 conditions of a critical bend radius relative to channel apex width, the imposed  
232 discharge, **and** the aggradation rate drive the development of cutoffs as indexed by  $M$ ,  
233 which reduces toward unity as the likelihood of cutoff becomes pronounced. This  
234 behavior develops independently of the presence of negligible bank-side vegetation.  
235 Thus, although vegetation can constrain planform, its presence is not a prerequisite to  
236 enable the wandering river planform to persist. By corollary, the behavior of other  
237 wandering rivers could be assessed in terms of cutoff criticality. Although channel  
238 behavior is explained by SOC, limitations remain; the detailed cutoff processes and  
239 how changes are transmitted beyond the cutoff locale require identification.

## 240 **CONCLUSIONS**

241       Low-sinuosity meanders on the Ganges River behaved similarly **to each other**  
242 **extending** over ~35 yr without downstream translation as sinuosity increased. Two  
243 meanders avulsed toward the end of the period, a third developed a soft avulsion, and  
244 the fourth was close to avulsion.

245       The critical bend radius-**to**-width ratio of  $\overline{1.29}$  was associated with avulsion.  
246 The role of super-elevation was accounted **for** in the avulsion process, but was small.

247 Rather, as shown for a barrage-effected meander, sinuosity increased once the  
248 backwater developed fully and aggradation drove the avulsion process.

249 Self-organized criticality, with a mobility number ( $M$ ) tracking meander  
250 development, showed that the critical **transition** is defined by  $M \approx 1$  when avulsion  
251 was imminent (Fig. 4). Channel phase space (Fig. 4) defined by Parker's braiding  
252 criterion and  $M$  demonstrates that the meander upstream of the barrage adjusted from  
253 an anastomosed braided system to a single-thread braided channel. Downstream, the  
254 system follows a wandering river trajectory varying through time from a meandering  
255 to an avulsive-anastomosed planform and then returns to meandering after  $\sim 35$  yr.

## 256 **ACKNOWLEDGMENTS (?)**

257 **[[Would you like to acknowledge s paper's reviewers (by name) in an**  
258 **Acknowledgments section?]]**

## 259 **REFERENCES CITED**

- 260 Bak, P., 1996, How Nature Works: **The Science of Self-Organized Criticality**: New  
261 York, Springer-Verlag, 212 p., doi:10.1007/978-1-4757-5426-1.
- 262 Begin, Z.B., 1986, Curvature ratio and rate of river bend migration—Update: Journal  
263 of Hydraulic Engineering, v. 112, p. 904–908, doi:10.1061/(ASCE)0733-  
264 9429(1986)112:10(904).
- 265 Braudrick, C.A., Dietrich, W.E., Leverich, G.T., and Sklar, L.S., 2009, Experimental  
266 evidence for the conditions necessary to sustain meandering in coarse bedded  
267 rivers: Proceedings of the National Academy of Sciences of the United States of  
268 America, v. 106, p. 16,936–16,941, doi:10.1073/pnas.0909417106.
- 269 Camazine, S., Deneubourg, J.-L., Franks, N., Sneyd, J., Theraulaz, G., and Bonabeau,  
270 E., 2001, Self-Organization in Biological Systems: Princeton, New Jersey,  
271 Princeton University Press, **[[Provide total number of pages]]**

- 272 Carson, M.A., 1984, Observations on the meandering-braided river transition,  
273 Canterbury Plains, New Zealand: Part two: *New Zealand Geographer*, v. 40,  
274 p. 89–99, doi:10.1111/j.1745-7939.1984.tb01044.x.
- 275 Chang, H.H., 1983, Energy expenditure in curved open channels: *Journal of*  
276 *Hydraulic Engineering*, v. 109, p. 1012–1022, doi:10.1061/(ASCE)0733-  
277 9429(1983)109:7(1012).
- 278 Church, M., 1983, Pattern of instability in a wandering gravel bed channel, *in*  
279 Collinson, J.D., and Lewin, J., eds., *Modern and Ancient Fluvial Systems*:  
280 International Association of Sedimentologists Special Publication 6, p. 169–180,  
281 doi:10.1002/9781444303773.ch13.
- 282 Coleman, J.M., 1969, Brahmaputra River: Channel processes and sedimentation:  
283 *Sedimentary Geology*, v. 3, p. 129–239, doi:10.1016/0037-0738(69)90010-4.
- 284 Edmonds, D.A., Hoyal, D.C.J.D., Sheets, B.A., and Slingerland, R.L., 2009,  
285 Predicting delta avulsions: Implications for coastal wetland restoration: *Geology*,  
286 v. 37, p. 759–762, doi:10.1130/G25743A.1.
- 287 Edmonds, D.A., Paola, C., Hoyal, D.C.J.D., and Sheets, B.A., 2011, Quantitative  
288 metrics that describe river deltas and their channel networks: *Journal of*  
289 *Geophysical Research*, v. 116, F04022, doi:10.1029/2010JF001955.
- 290 Germanoski, D., and Schumm, S.A., 1993, Changes in braided river morphology  
291 resulting from aggradation and degradation: *The Journal of Geology*, v. 101,  
292 p. 451–466, doi:10.1086/648239.
- 293 Hooke, J.M., 2007, Complexity, self-organisation and variation in behaviour in  
294 meandering rivers: *Geomorphology*, v. 91, p. 236–258,  
295 doi:10.1016/j.geomorph.2007.04.021.

- 296 Hossain, M.A., Gan, T.Y., Basar, A., and Baki, M., 2013, Assessing morphological  
297 changes of the Ganges River using satellite images: *Quaternary International*,  
298 v. 304, p. 142–155, doi:10.1016/j.quaint.2013.03.028.
- 299 Howard, A.D., 2009, How to make a meandering river: *Proceedings of the National*  
300 *Academy of Sciences of the United States of America*, v. 106, p. 17,245–17,246,  
301 doi:10.1073/pnas.0910005106.
- 302 Howard, A.D., and Knutson, T.R., 1984, Sufficient conditions for river meandering:  
303 A simulation approach: *Water Resources Research*, v. 20, p. 1659–1667,  
304 doi:10.1029/WR020i011p01659.
- 305 Jerolmack, D.J., and Mohrig, D., 2007, Conditions for branching in depositional  
306 rivers: *Geology*, v. 35, p. 463–466, doi:10.1130/G23308A.1.
- 307 Kasvi, E., Vaaja, M., Kaartinen, H., Kukko, A., Jaakkola, A., Flener, C., Hyyppä, H.,  
308 Hyyppä, J., and Alho, P., 2015, Sub-bend scale flow–sediment interaction of  
309 meander bends—A combined approach of field observations, close-range remote  
310 sensing and computational modelling: *Geomorphology*, v. 238, p. 119–134,  
311 doi:10.1016/j.geomorph.2015.01.039.
- 312 Leopold, L.B., Bagnold, R.A., Wolman, M.G., and Brush, L.M., 1960, Flow  
313 resistance in sinuous or irregular channels: *U.S. Geological Survey Professional*  
314 *Paper 282-D*, p. 111–134.
- 315 Parker, G., 1976, On the cause and characteristic scales of meandering and braiding in  
316 rivers: *Journal of Fluid Mechanics*, v. 76, p. 457–480,  
317 doi:10.1017/S0022112076000748.
- 318 Prokopenko, M., Polani, D., and Ay, N., 2014, On the cross-disciplinary nature of  
319 guided self-organization, *in* Prokopenko, M., ed., *Guided Self-Organization:*  
320 *Inception*: New York, Springer, p. 3–15, doi:10.1007/978-3-642-53734-9\_1.

- 321 Seminara, G., 2006, Meanders: *Journal of Fluid Mechanics*, v. 554, p. 271–297,  
322 doi:10.1017/S0022112006008925.
- 323 Sorrells, R.M., and Royall, D., 2014, Channel bifurcation and adjustment on the upper  
324 Yadkin River, North Carolina (USA): *Geomorphology*, v. 223, p. 33–44,  
325 doi:10.1016/j.geomorph.2014.06.020.
- 326 Stølum, H.-H., 1996, River meandering as a self-organization process: *Science*,  
327 v. 271, p. 1710–1713, doi:10.1126/science.271.5256.1710.
- 328 Stølum, H.-H., 1998, Planform geometry and dynamics of meandering rivers:  
329 *Geological Society of America Bulletin*, v. 110, p. 1485–1498, doi:10.1130/0016-  
330 7606(1998)110<1485:PGADOM>2.3.CO;2.
- 331 van Dijk, W.M., Schuurman, F., van de Lageweg, W.I., and Kleinans, M.G., 2014,  
332 Bifurcation instability and chute cutoff development in meandering gravel-bed  
333 rivers: *Geomorphology*, v. 213, p. 277–291,  
334 doi:10.1016/j.geomorph.2014.01.018.
- 335 Wasson, J., 2003, A sediment budget for the Ganga–Brahmaputra catchment: *Current*  
336 *Science*, v. 84, p. 1041–1047.
- 337 Wu, B., Zheng, S., and Thorne, C.R., 2012, A general framework for using the rate  
338 law to simulate morphological response to disturbance in the fluvial system:  
339 *Progress in Physical Geography*, v. 36, p. 575–597,  
340 doi:10.1177/0309133312436569.

341 **FIGURE CAPTIONS**

342 Figure 1. **Development of** Ganges River meanders R1–R4 in A.D. 1972–2011. **Inset:**  
343 **Location map showing study area.**

344

345 Figure 2. A: Derivation of maximum channel aggradation rate, Ganges River, India.  
346 Triangles show years ( $Y$ ) of aggradation; squares are years after Farakka Barrage was  
347 full. B: Sinuosity of the R1 meander over time. “Full”**[[Explain the need for**  
348 **quotation marks (i.e., what is meant by “full”)]** channel ~~aggradation~~ accelerates  
349 meander sinuosity.**[[In the figure, panel B, it is not clear what is meant by “Years**  
350 **of change in Base Level” – do you mean “Year” (regular, as in calendar year)?**  
351 **(Also, “Change” should be capitalized for consistency)]**

352

353 Figure 3. Mobility number and sinuosity versus year for Ganges River meanders.  
354 Circles are mobility number ( $M$ ) fitted with polynomial functions; squares are  
355 sinuosity of main channel; triangles are cutoff sinuosity. Black arrows are cutoff  
356 initiation dates; white arrow is date of cutoff failure (see Fig. 1).

357

358 Figure 4. Channel pattern phase space: AB—anastomosed-braided; BS—braided-  
359 single; AW—wandering; S—sinuous-single. Time trends, labeled with calendar years  
360 A.D., are shown for Ganges River meanders R1 and R4.